

Research Article

# Flexural Analysis of Butt-Joint Prepared by CFRP Windings between two Aluminium Adherend Pipes using ANSYS.

Shailesh L. Deshmukh\*, Prashant Kumar, R. N. Ladhav and Prashant Patane

\*Department of Mechanical Engineering, MIT COE, Savitribai Phule Pune University, Pune, India

Accepted 02 March 2016, Available online 15 March 2016, **Special Issue-4 (March 2016)**

## Abstract

A FRP butt-joint was developed between two adherends of aluminium pipes of outside diameter 25.5 mm, inside diameter 22 mm and length 175 mm. The joint was formed by winding wetted roving of carbon fiber with controlled quantity of epoxy at  $\pm 45^\circ$  angle. It was cured to form the joint with CFRP working as a sleeve. The joint was simulated using ANSYS software, for two kinds of loading i) tensile loading and ii) flexural loading. Under a four point bend test with thin CFRP sleeve ( $n = 80$ ), the failure occurred at the maximum load of 3470 N, due to breakage of CFRP at the joint plane. When the CFRP sleeve was made thicker ( $n=150$ ), the aluminium adherend failed due to formation of plastic hinges in the aluminium adherends outside the CFRP sleeve.

**Keywords:** FRP, adherends, Flexural, CFRP, ANSYS etc.

## 1. Introduction

The word composite means, "consisting of two or more distinct phases". Thus materials having two or more distinct constituents, having distinct interface separating them are called composite materials. Polymer composites are an important class of composite material in which a polymer is reinforced by stiff and high strength fibers. They have proven properties in number of engineering fields such as aerospace, automotive and civil engineering. The reason for their getting more popular day-by-day is that they accommodate desirable properties like lightweight, high stiffness to weight and strength to weight characteristics and good corrosion resistance. The reinforcing fiber or fabric provides strength and stiffness to the composite, whereas matrix gives rigidly and environmental resistance. The properties strongly depend on the way the fibers are laid in the composites. The important thing to remember about composites is that fiber carries the load and its strength is greatest along the axis of the fiber. When investigating the use of fiber reinforced plastic (FRP) piping in the chemical, petrochemical, marine, and other industries, several decisions have to be made early on in the design of the piping system. These include the fabrication technique (filament winding vs hand-layup, for example), the method of installation and the joining system (adhesive-bonded v/s butt and strap, for example), to name a few. The joining method used in a piping system can often determine the

success or detriment of the system over its years of use, thus making it one of the more important factors in the engineering design of the system. Fiber Reinforced Polymers (FRP) is now being accepted as an important class of 'engineered materials', because it offers several outstanding properties. People are exploring the application of polymer composites in various different directions.

This is but one of the many aspects of FRP piping systems that must be investigated before a successful design can be completed. Fabrication materials, pipe flexibility, and pipe strength are but a few of the additional aspects that should be considered. By reading and understanding the information in this report, one step of many is taken toward the successful design of a FRP in piping system. Different types of joining methods are available to join two or more similar or dissimilar materials. They can be classified as:

- (i) Fasteners (such as threaded bolts, rivets, etc.).
- (ii) Welding, brazing or soldering.
- (iii) Adhesive bonding.
- (iv) Tying components together.
- (v) Stitching.
- (vi) Gripping through elastic deformation (interference fit, spring loaded clips, etc).
- (vii) Using magnetic force for joining.

Each of these techniques has its own advantages and limitations. A new method is recently developed by [Kumar P. (2008)], in which, composites are used to join two parts together with a FRP material. In the FRP joint, the composite which acts as an adhesive is made

\*Corresponding author: **Shailesh L. Deshmukh**

of strong fibers (glass, carbon, Kevlar), and a thermoset matrix (epoxy, polyester). To make a FRP joint the reinforcement is wetted in a thermosetting resin (epoxy, polyester, etc.) and wound on the joint and the resin is allowed to get cured. A FRP joint offers numerous advantages.

- The joining can be easily done at room temperature, as it is a cold working process.
- This method can be used to join similar or dissimilar materials. This overcomes the limitations of welding in which similar or certain pairs of materials can only be joined.
- This provides non-corrosive joint.
- It is a simple technique and hence does not require much skilled labor.
- If the joint is not made properly, the adherends can be recovered easily and again joined by a FRP material. Hence this method does not harm the adherends even after detachment.
- The FRP joint offers high strength to weight ratio.
- It is economical.

Due to these several advantages offered by FRP, now-a-days, FRP is being used in several industrial applications. Some of them are listed below:

- Aircrafts
- Auto body
- Auto frame
- Bridge reinforcement
- Shafts and rods, etc.

The components of these structures can be joined through FRP.

## 2. Objectives

The objective of the present study was to simulate and analyze a CFRP butt joint for flexural test. The simulation is carried out by using ANSYS software. The present work is distributed in the following ways.

Specimen preparation.' describes the experimental method used for development of specimen of CFRP butt joint.

Experimental techniques' describes the test methods for flexural test used to carry out experiments on the specimens.

Numerical techniques' gives, details about modeling, meshing, boundary conditions used in ANSYS to simulate flexural test.

CFRP flexural test results and discussion' describe numerical results obtained from ANSYS software for the flexural test.

Conclusion describes the conclusion on numerical results for flexural test. Also gives scope for future work.

## 3. Specimen and FRP Winding method

To wind the wetted CFRP, an effective winding configuration was developed to prepare the specimen.

Three kinds of winding angles were employed,  $\pm 45^\circ$ ,  $70^\circ$  and  $90^\circ$  (C loops) as shown in Figure 3.1. Winding of  $\pm 45^\circ$  and  $\pm 70^\circ$  were running winding from one adherend to another. It was important to develop adequate adhesion between the adherends and the CFRP sleeve. After many alternative trial and errors, it was found that good adhesion was developed when the end points of running winding was pressed by two local loops of  $90^\circ$  winding. Passes of  $\pm 45^\circ$  winding, played a major role in the CFRP joint, but it was found that four passes initially of  $\pm 70^\circ$  winding were helpful in enhancing the adhesion. Thus, the four passes of  $70^\circ$  winding constituted the preparatic winding over which main winding of  $\pm 45^\circ$  was carried out. The configuration of the preparatic winding was  $[90_2/70/90_2/-70]_4$ . The configuration of the main winding was  $[90_2/45/90_2/-45]_n$  in which n was large number and was varied in the characterization of the CFRP joint. The winding thus formed a CFRP sleeve of about 130 mm long.

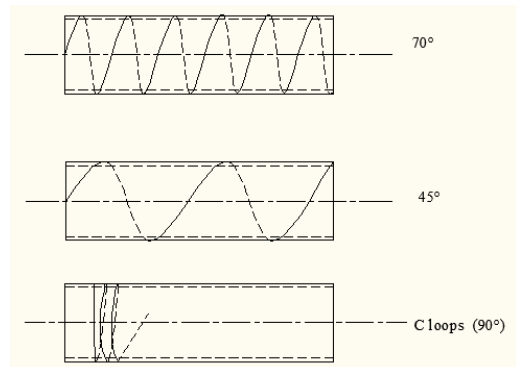


Figure 3.1:  $70^\circ$ ,  $45^\circ$  and c-loops of winding

The wetted roving carbon fiber was wound on the specimen on the center portion of the length about 130 mm. The schematic diagram of the specimen is shown in Figure 2.1 and the photograph of a specimen is represented in Figure 3.2.

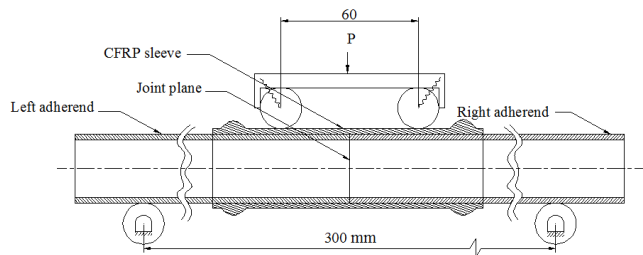


Figure 3.2 Photograph of the CFRP butt-joint

## 4. Experimentation

For characterizing the CFRP butt joint, flexure tests were performed on a 10 ton capacity Universal Testing Machine. The schematic diagram of flexural test set-up is as shown in the Figure 3.1 and the photograph of actual test set-up is shown in the Figure 3.2. The distance between the two central loads was chosen to be small (only 60mm). This was done (i) to increase the bending moment at the joint plane and (ii) the load

points of the center loads acted on the FRP sleeve which is quite strong and as a result it did not cause any local plastic deformation.



**Figure 4.1** The schematic diagram of four-point-bend test set-up



**Figure 4.2** Photograph of the flexural loading

**5. Numerical Techniques**

In this study, the numerical analysis was done by using ANSYS 13.0 so that results can be compared and checked. The various stresses axial, shear, radial etc. near the interface of two materials can be easily found out by using this numerical analysis.

*Properties of aluminium adherend*

Aluminium adherend was deformed as elastic-plastic material. The material properties of aluminium adherend were determined through an experiment by pulling the aluminium tube through a 10 ton UTM. The stress strain relation is shown in Figure 5.1, Rajesh Sabne [2012]. The Yield Stress of aluminium adherend was 210 MPa and Ultimate Tensile Strength (UTS) of aluminium adherend was 249.5 MPa [Sabne R. S.]. Both linear isotropic as well as non-linear material properties i.e. stress and strain values were provided for analysis. The non-linear isotropic properties of aluminium adherend provided for the analysis are given in Table 5.1

*Linear isotropic properties of aluminium adherend*

Modulus of (EX) = 56,942 MPa  
 Poissons ratio (NUXY) = 0.3

**Table 5.1:** The non-linear isotropic properties of aluminium adherend

Sr. No	Stress (MPa)	Strain
1	182.1	0.003198
2	203.6	0.004398
3	215.2	0.01372
4	222.3	0.03968
5	226.7	0.05844
6	230.8	0.07836
7	234	0.09528

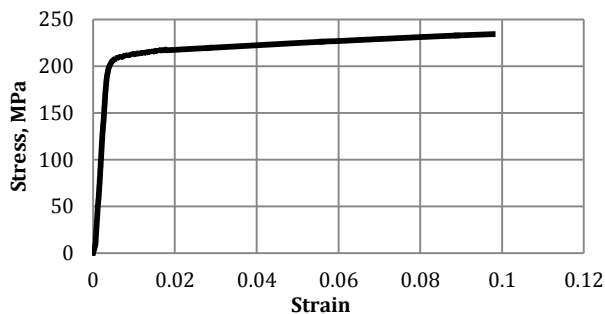


**Figure 5.1** Stress strain curve for aluminium adherend

*Properties of Epoxy*

Epoxy was considered as linear isotropic material and its properties are given below,  
 Modulus (EX) = 3.35 GPa.

Poissons ratio (NUXY) = 0.36

*Properties of CFRP*

FRP was considered as linear anisotropic elastic material. The values of elastic constants in MPa, along the global axes direction, for  $\theta = +45^\circ$ ,  $\theta = -45^\circ$ ,  $\theta = +70^\circ$  and  $\theta = -70^\circ$  are given in Table 5.2

**Table 5.2:** Elastic constants in MPa along global axes direction

	$\theta = +45^\circ$	$\theta = -45^\circ$	$\theta = +70^\circ$	$\theta = -70^\circ$
D11	30232	30232	11201	11201
D12	25192	25192	12821	12821
D13	3769	3769	3507	3507
D14	0	0	0	0
D15	0	0	0	0
D16	20496	-20496	2794	-2794
D22	30232	30232	74007	74007
D23	3769	3769	4030	4030
D24	0	0	0	0
D25	0	0	0	0
D26	20496	-20496	23555	-23555
D33	10321	10321	10321	10321
D34	0	0	0	0
D35	0	0	0	0
D36	341.8	-341.8	219.7	-219.7
D44	2520	2520	2520	2520
D45	0	0	0	0
D46	0	0	0	0
D55	2520	2520	2520	2520
D56	0	0	0	0
D66	23602	23602	11230	11230

## 6. Geometry for flexural test specimen

### 6.1 For thin sleeve specimen

The specimen with 80 numbers of passes of  $\pm 45^\circ$  windings was chosen for analysis R. S. Sabne (2012). The gap between two ends of aluminium adherends was taken to be small only 20 microns. The thicknesses of aluminium adherends, epoxy layer, 70 degree layers and FRP layers (+45 and -45 degree layers) used for modelling were 1.66 mm, 0.1 mm, 0.2 mm and 0.8 mm respectively. For the analysis for flexural test, full model was used.

### 6.2 For thick sleeve specimen

For thick sleeve analysis, the specimen with 150 numbers of passes of  $\pm 45^\circ$  windings was chosen for analysis R. S. Sabne (2012). The gap between two ends of aluminium adherends was taken to be small only 20 microns. The thicknesses of aluminium adherends, epoxy layer, 70 degree layers and FRP layers (+45 and -45 degree layers) used for modelling were 1.66 mm, 0.1 mm, 0.2 mm and 1.5 mm respectively. For the analysis for flexural test, full model was used.

### 6.3 Software details for flexural test

#### Element used

For flexural test (four points bend test) solid 186 and solid 185 elements are used. Solid 186 is a higher order 3-D 20-noded solid element that exhibits quadratic displacement behaviour. Solid 185 is a 3-D 8-noded solid element. These elements are having three degrees of freedom per node: translations in the nodal x, y, and z directions. Both these element supports plasticity, hyper elasticity, creep, stress stiffening, large deflection, and large strain capabilities. They also have mixed formulation capability for simulating deformations of nearly incompressible elasto plastic materials, and fully incompressible hyper elastic materials.

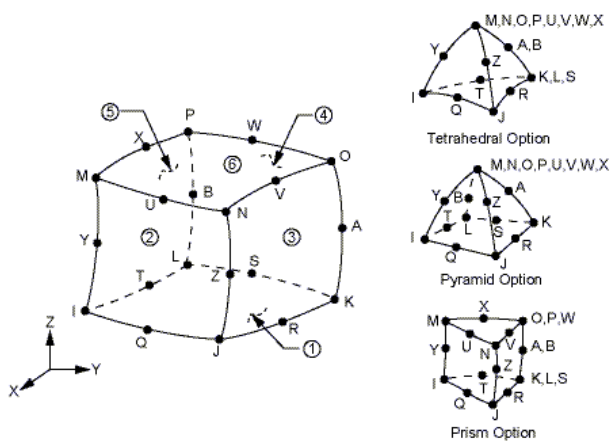


**Figure 6.1** Solid 186 homogeneous structural solid geometry and its optional shape

### 6.4 Meshing

Solid 186 which is 20 noded, elements was used near joint plane for the distance of 10 mm from each side of JP and for remaining portion, solid 185 which is 8 noded, elements was used. Figure 6.2 gives meshing details for flexural test.

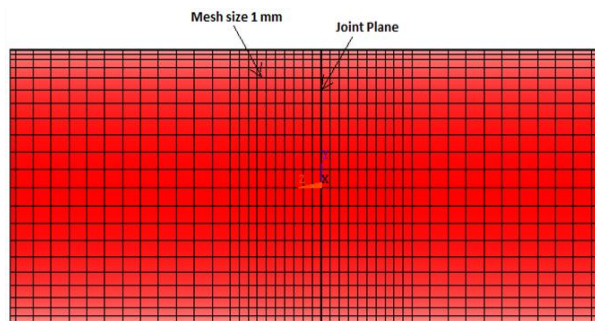


**Figure 6.2** Meshing details for flexural test

### 6.5 Boundary conditions used for flexural test

For thin sleeve specimen, the flexural load of 1735 N was applied by selecting the nodes at a distance of 30 mm from each side of joint plane, R.S. Sabne (2012). The cylindrical co-ordinates system (csys,1-command) was used for selection of nodes. For displacement boundary conditions, the nodes at a distance of 150 mm from each side of JP were selected. The displacement boundary conditions used was  $U_x = 0$ ,  $U_y = 0$  on each side of JP. Also  $U_z = 0$ , was provided at only one lower portion node, so that the whole model was firmly tied in space.

For thick sleeve specimen, the loading and displacement boundary conditions were similar to those used for thin sleeve specimen under flexural load, except a flexural load of 2600 N was applied at each side of JP.

## 7. Results and Discussions

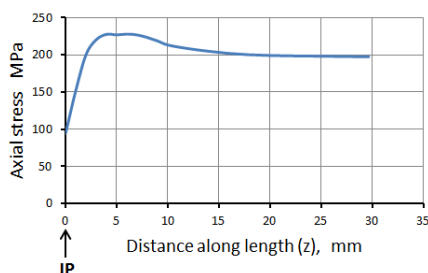
### 7.1 Numerical Analysis of Flexural Test For Thin Sleeve Specimen

The failure of the CFRP thin specimen under flexural loading which is a four point bend test is explained in this section. The specimen with 80 numbers of passes of  $\pm 45^\circ$  FRP windings was chosen for analysis. The results obtained through the numerical technique are discussed here. The model used in ANSYS consists of aluminium adherends of wall thickness 1.6 mm, epoxy and  $\pm 70^\circ$  FRP layers of thickness 0.1 mm each and  $\pm 45^\circ$  FRP layers of thickness 0.8 mm. The meshing of the model is explained in Section 4.4 It is worth noting that aluminium thickness is divided into 8 concentric layer and also  $\pm 45^\circ$  FRP thickness is divided into 8 layers. Near JP element length of 1 mm was used in z direction. Analysis was carried out under flexural load of 3470 N. The loading and boundary conditions for this model have been discussed in previous section.

The ANSYS 13.0, a finite element method based software was used for the analysis. The elastic - plastic behavior of aluminium adherend was used and the software uses Newton - Raphson technique for nonlinear solution. For the analysis, linear elastic limit ( $\sigma_e$ ) of aluminium was taken to be 188 MPa beyond which aluminium material starts yielding. Invoking numerical analysis for tensile thin and thick sleeve specimen, the yield stress of aluminium was 210 MPa, but for numerical analysis, yield point is just one point of the plastic deformation. The ultimate tensile strength( $\sigma_{uts}$ ) of aluminium adherend was 249.5 MPa. In this numerical analysis, axial stress  $\sigma_{zz}$ , shear stress  $\sigma_{rz}$  developed during four point bend test, was dominant stress. Therefore, they are discussed first. Other stress component radial stress  $\sigma_{rr}$  is small compared to  $\sigma_{zz}$  and it is discussed subsequently.

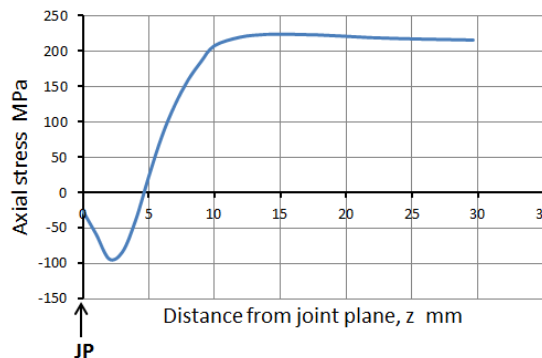
*Axial stress  $\sigma_{zz}$*

Figure 7.1 gives the axial stress  $\sigma_{zz}$  developed in aluminium adherend at the tension side of model close to its interface with thin epoxy layer. At JP,  $\sigma_{zz}$  of 98 MPa was developed and it reached a peak of 227 MPa at the distance of 4 mm from JP. After that it was decreased to 200 MPa at the distance of 16 mm from JP. Theoretically, in four point bend test, constant bending moment developed between the inner two rollers through which load was applied on specimen (in this case 30 mm from JP). However, aluminium tube was not continuous, giving rise to varying  $\sigma_{zz}$  along the length. From numerical analysis, it was found that  $\sigma_{zz}$  at a short distance from JP was quite high. It cause plastic deformation, but was not high enough to cause its failure ( $\sigma_{uts} = 249.5$  MPa). Similar to the result of the tensile test with thin CFRP sleeve, stress becomes higher than the stabilized  $\sigma_{zz} = 200$  MPa about 17 mm from JP. Since the portion of aluminium tube was not supported underneath, some pinching effect was present. This effect is supported by Figure 7.2 which shows  $\sigma_{zz}$  at the interior surface of aluminium tube. Close to JP, stresses were compressive but soon became tensile beyond  $z = 12$  mm.



**Figure 7.1** Axial stress ( $\sigma_{zz}$ ) at aluminium adherend at its outer surface just below epoxy layer

Figure 7.3 shows the axial stress within epoxy layer close to its interface with aluminium surface. At JP  $\sigma_{zz}$  of 398 MPa was found in thin epoxy layer. The  $\sigma_{zz}$  was gradually decreased to 28 MPa at a distance of 10 mm from JP. The epoxy was expected to fail at this high  $\sigma_{zz}$ .



**Figure 7.2** Axial stress  $\sigma_{zz}$  at inner surface aluminium

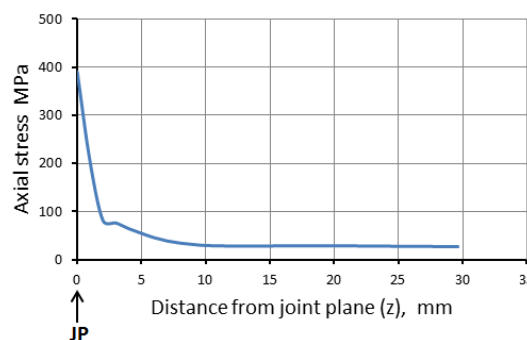


**Figure 7.3** Axial stress  $\sigma_{zz}$  at epoxy surface

Axial stress  $\sigma_{zz}$  in  $\pm 70^\circ$  FRP layer is shown in Figure 7.4. The maximum  $\sigma_{zz}$  was found as 380 MPa at the JP.  $70^\circ$  layer could not take this high stress and probably it would also fail at JP. However the layer is so small that its failure would not cause much readjustment of stresses.

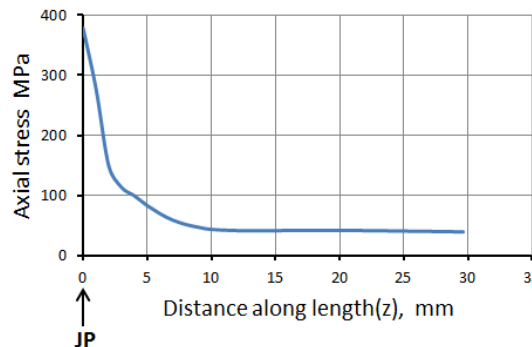


**Figure 7.4** Axial stress  $\sigma_{zz}$  at  $\pm 70^\circ$  layer surface (at mid thickness)

Figure 7.5 shows  $\sigma_{zz}$  developed through the thickness of  $\pm 45^\circ$  FRP layer. Near JP maximum axial stress of 223 MPa was observed at outer surface of FRP ( $R = 13.8$  mm). It was 210 MPa at the radius of 13.6 mm. Since  $\pm 45^\circ$  layers as discussed earlier, fails at the ultimate strength of 220 MPa, the FRP sleeve started breaking from its outer surface. Once the outer layer failed, the inner portion of  $\pm 45^\circ$  CFRP sleeve would be subjected to higher  $\sigma_{zz}$ . Thus the numerical analysis predicted that CFRP thin sleeve started failing at its outer surface at JP. The failure extended to inner layers of FRP till it failed completely.

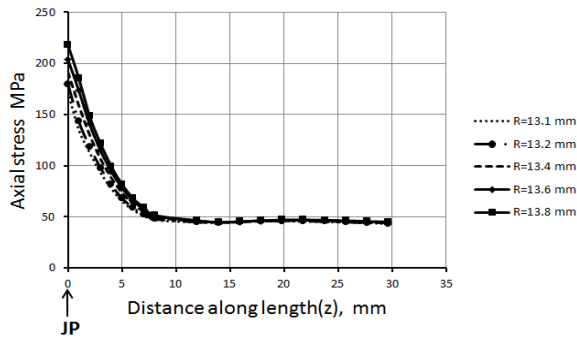
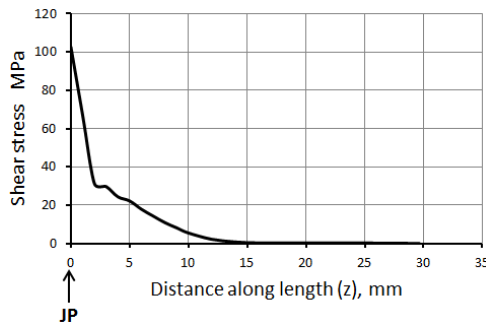


**Figure 7.5** Axial stress  $\sigma_{zz}$  through the thickness of at  $\pm 45^\circ$  FRP layer

*Shear stress  $\sigma_{rz}$*

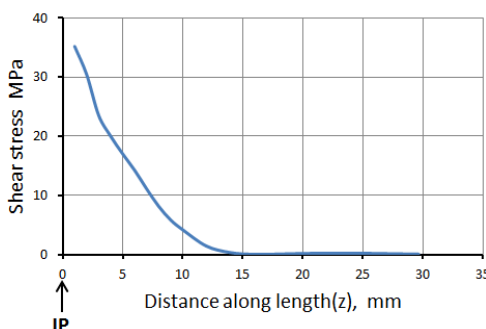
During flexural test the applied load was transferred from aluminium adherend to CFRP sleeve by means of shear stress. The interface of aluminium and epoxy plays a vital role to transfer load from aluminium to CFRP sleeve. Also the shear stress at the interface of epoxy and  $\pm 70^\circ$  FRP layer, between  $\pm 45^\circ$  and  $\pm 70^\circ$  FRP layer was also discussed.

Figure 7.6 gives the shear stress  $\sigma_{rz}$  at the interface of aluminium and epoxy. At JP,  $\sigma_{rz}$  of 100 MPa was found. Epoxy could not resist such high  $\sigma_{rz}$  near JP. Probably epoxy would fail in shear but CFRP fails at JP due to high axial stress.



**Figure 7.6** Shear stress  $\sigma_{rz}$  at the interface of aluminium and epoxy surface

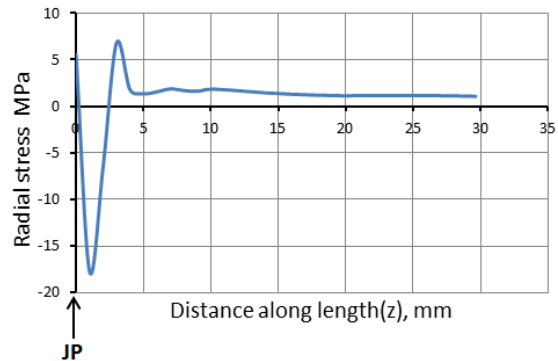
Figure 7.7 shows the shear stress  $\sigma_{rz}$  at the interface of  $\pm 70^\circ$  and  $\pm 45^\circ$  layers. The value of  $\sigma_{rz}$  at JP was 35 MPa and it became zero at a distance of 15 mm from JP. It was small and would not cause delamination.



**Figure 7.7** Shear stress  $\sigma_{rz}$  at the interface of  $\pm 70^\circ$  and  $\pm 45^\circ$  layers

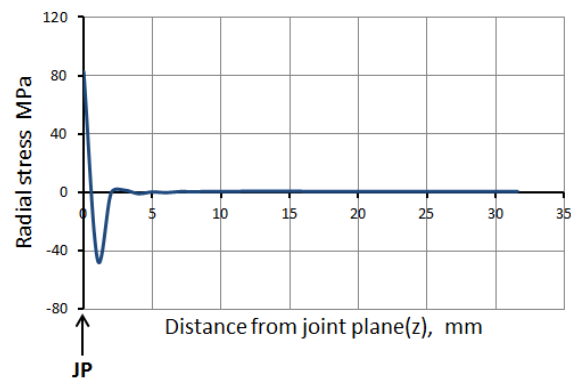
*Radial stress  $\sigma_{rr}$*

Figure 7.8 shows the radial stress  $\sigma_{rr}$  developed at the interface of aluminium and epoxy surface. The  $\sigma_{rr}$  was 5 MPa at JP. It was compressive of peak -18 MPa at a distance of 1.5 mm from JP and it became tensile having peak of 7 MPa. This was probably due to the local bending of aluminium near JP.



**Figure 7.8** Radial stress  $\sigma_{rr}$  at the interface of aluminium and epoxy surface

The radial stress at the interface of  $\pm 70^\circ$  and  $\pm 45^\circ$  FRP layer is shown in Figure 7.9. At the JP,  $\sigma_{rr}$  was 82 MPa and changes to compressive of -45 MPa at a distance of 2 mm from JP. Beyond 3 mm from JP  $\sigma_{rr}$  became zero.



**Figure 7.9** Radial stress  $\sigma_{rr}$  at the interface of  $\pm 70^\circ$  and  $\pm 45^\circ$  FRP layer

*7.2 Numerical analysis of flexural test for thick*

The failure of the CFRP thick sleeve specimen under flexural loading which is a four point bend test is explained in this section. For thick sleeve flexural test, the specimen with 150 numbers of passes of  $\pm 45^\circ$  FRP windings was used for analysis. The results obtained through the numerical technique are discussed here. The geometric model used in ANSYS for thick sleeve is similar to as used for thin sleeve, except the thickness of  $\pm 45^\circ$  FRP layers which is 1.5 mm for thick sleeve. The meshing of the model is explained in section 4.3.2. It is worth noting that aluminium thickness is divided into 8 concentric layer and  $\pm 45^\circ$  FRP thickness is also

divided into 8 layers. Near JP, element length of 1 mm was used in z direction. Analysis was carried out under flexural load of 5200 N. The loading and boundary conditions for this model are similar to those used for thin sleeve.

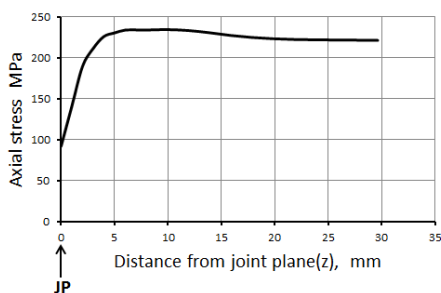
The ANSYS 13.0, a finite element method based software was used for analysis. The nature of solution was nonlinear as elastic – plastic behavior of aluminium adherends was considered and solver uses the Newton Raphson method by default. For this analysis, linear elastic limit ( $\sigma_e$ ) of aluminium was taken to be 188 MPa from where aluminium starts yielding. Invoking the stress strain curve for aluminium adherend, the yield stress of aluminium was 210 MPa and its ultimate tensile strength was 249.5 MPa.

In this numerical analysis the flexural or axial stress  $\sigma_{zz}$  developed during four point bend test was dominant stress; therefore, it is discussed first. Other stress components, shear stress  $\sigma_{rz}$  and radial stress  $\sigma_{rr}$ , are small as compared to  $\sigma_{zz}$  are discussed subsequently. The results are given at the bottom side (tension side) of the specimen.

*Axial stress  $\sigma_{zz}$*

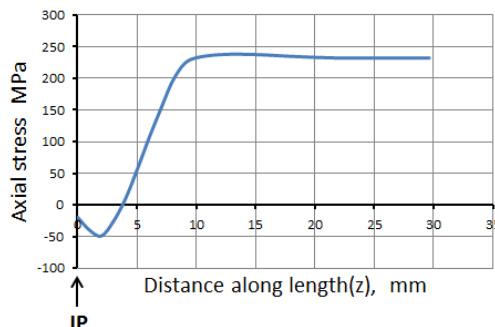
Figure 7.10 shows the axial stress  $\sigma_{zz}$  developed in aluminium adherend at the tension side (bottom portion) of model close to the interface with thin epoxy layer. At the JP  $\sigma_{zz}$  of 92 MPa was developed and it reached a peak of 234 MPa at the distance of 9 mm from JP. The ultimate tensile strength of aluminium adherend used is 249.5 MPa. After that it was reduced to 222 MPa at the distance of 22 mm from JP. Theoretically in four point bend test, constant bending moment developed between the two rollers through which load was applied on specimen (in this case 30 mm from JP). From numerical analysis it was found that near JP aluminium crosses the elastic limit ( $\sigma_e = 188$  MPa). Also  $\sigma_{zz}$  was greater than yield stress of aluminium ( $\sigma_{yst} = 210$  MPa). Therefore yielding of aluminium adherend took place near JP.

Also the shear stress  $\sigma_{rz}$  at the interface between aluminium adherend and epoxy layer was found as 100 MPa near JP (Figure 7.18). These two high stresses  $\sigma_{zz}$  and  $\sigma_{rz}$  near JP probably causes the failure of aluminium and epoxy interface and aluminium adherend would separates from FRP at JP.



**Figure 7.10** Axial stress ( $\sigma_{zz}$ ) in aluminium adherend at its outer surface (on the tensile side), just below epoxy layer

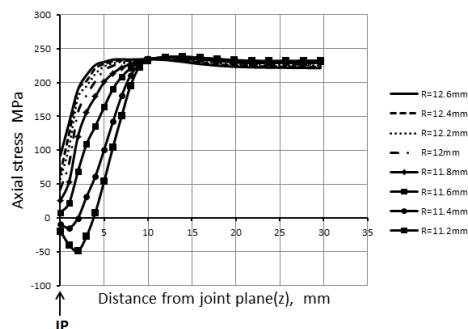
The axial stress  $\sigma_{zz}$  at the inner surface of aluminium is shown in Figure 7.13. At the JP a compressive stress of 19 MPa was observed and it became tensile after 4 mm from JP. At a distance of 12 mm from JP, the  $\sigma_{zz}$  took the peak of 223 MPa, greater than yield stress of aluminium adherend.



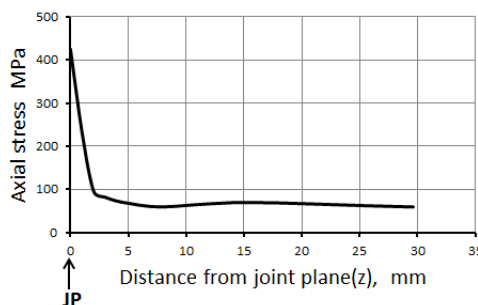
**Figure 7.11** Axial stress  $\sigma_{zz}$  at inner surface of aluminium adherend

The axial stress  $\sigma_{zz}$  through the thickness of aluminium adherend is shown in Figure 7.12. Close to inner surface,  $\sigma_{zz}$  for the radius of 11.2 mm and 11.4 mm was compressive at JP and it became tensile for larger radius. This was because local bending of aluminium occurring near JP. The  $\sigma_{zz}$  at the distance of 9 mm from JP, was greater than its elastic limit ( $\sigma_e \approx 188$  MPa) through the thickness of adherend. This numerical analysis showed that, plastic deformation of aluminium adherend took place throughout its thickness.

Figure 7.13 shows the axial stress developed within epoxy layer. At JP,  $\sigma_{zz}$  of 425 MPa was found in thin epoxy layer. The  $\sigma_{zz}$  was gradually decreased to 95.6 MPa at a distance of 2 mm from JP. The epoxy was expected to fail due to this high  $\sigma_{zz}$ .

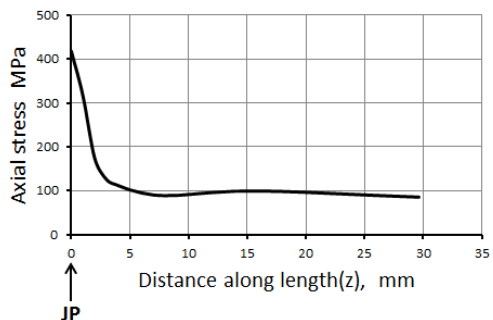


**Figure 7.12** Axial stress  $\sigma_{zz}$  through the thickness of aluminium adherend



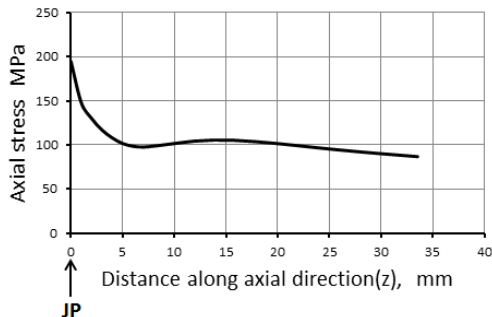
**Figure 7.13** Axial stress  $\sigma_{zz}$  within thin epoxy layer

Axial stress  $\sigma_{zz}$  in  $\pm 70^\circ$  FRP layer is shown in Figure 7.14. The maximum  $\sigma_{zz}$  was found as 415 MPa at the JP and it was gradually decreased to 100 MPa at a distance of 5 mm from JP. The  $\pm 70^\circ$  layer could not take this high stress and probably it would fail at J.P.



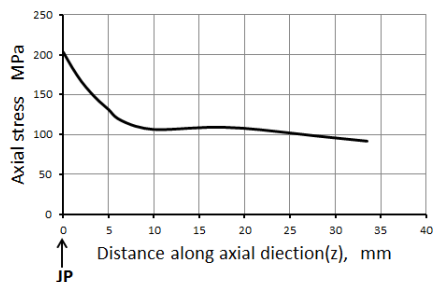
**Figure 7.14** Axial stress  $\sigma_{zz}$  at  $\pm 70^\circ$  layer surface (at mid thickness)

Figure 7.15 shows  $\sigma_{zz}$  developed in  $\pm 45^\circ$  FRP layer just outside of  $\pm 70^\circ$  FRP layer. Near the JP  $\sigma_{zz}$  was 193 MPa. It was gradually decreased to 104 MPa at the distance of 10 mm from JP. The  $\sigma_{zz}$  was not high enough to cause failure of  $\pm 45^\circ$  FRP layer.



**Figure 7.15** Axial stress  $\sigma_{zz}$  at  $\pm 45^\circ$  FRP layer just below  $\pm 70^\circ$  FRP layer

The axial stress  $\sigma_{zz}$  at outer of FRP sleeve is shown in Figure 7.16. Near JP  $\sigma_{zz}$  of 203 MPa was observed, which was less than tensile strength of CFRP sleeve ( $\approx 220$  MPa) for  $\pm 45^\circ$  windings. It was gradually decreases to 105 MPa at the distance of 10 mm from JP.



**Figure 7.16** Axial stress  $\sigma_{zz}$  at outer of FRP sleeve

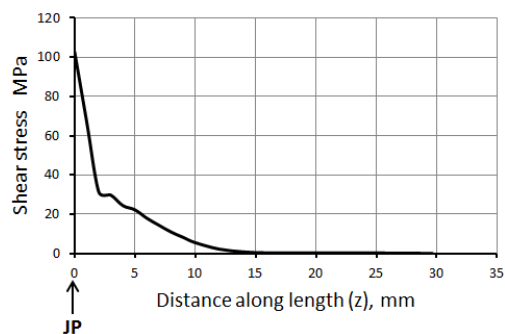
*Shear stress  $\sigma_{rz}$*

During flexural test the applied load was transferred from aluminium adherend to CFRP sleeve by means of

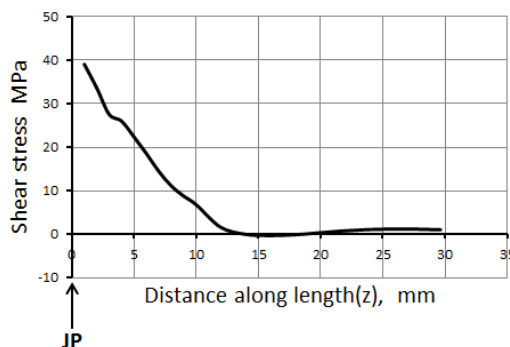
shear stress. The interface of aluminium and epoxy plays a vital role to transfer a load from aluminium to CFRP sleeve. Also the shear stress at the interface of epoxy and  $\pm 70^\circ$  FRP layer, between  $\pm 45^\circ$  and  $\pm 70^\circ$  FRP layer was discussed.

Figure 7.17 gives the shear stress  $\sigma_{rz}$  at the interface of aluminium and epoxy. At the JP,  $\sigma_{rz}$  of 102 MPa was found. Epoxy couldn't resist such high  $\sigma_{rz}$  near JP. Probably epoxy would break. Due to this high  $\sigma_{rz}$  at the aluminium and epoxy interface, probably aluminium separates out from FRP near JP. Thus, the numerical analysis predicts that separation of aluminium adherend took place near JP.

Figure 7.18 shows the shear stress  $\sigma_{rz}$  at the interface of  $\pm 70^\circ$  and  $\pm 45^\circ$  layers. The value of  $\sigma_{rz}$  at JP was 38 MPa and it became zero at a distance of 15 mm from JP.



**Figure 7.17** Shear stress  $\sigma_{rz}$  at the interface of aluminium and epoxy surface

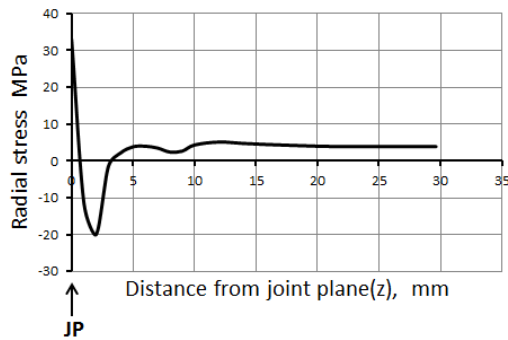


**Figure 7.18** Shear stress  $\sigma_{rz}$  at the interface of  $\pm 70^\circ$  and  $\pm 45^\circ$  layers

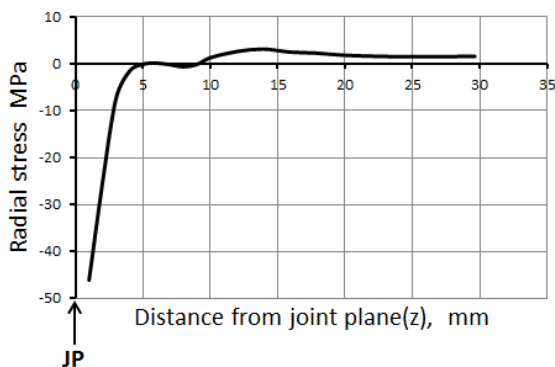
*Radial stress  $\sigma_{rr}$*

Figure 7.19 shows the radial stress  $\sigma_{rr}$  developed at the interface of aluminium and epoxy surface. The  $\sigma_{rr}$  was 32 MPa at JP. It was compressive of -20 MPa at a distance of 1.5 mm from JP and it became tensile having peak of 5 MPa. This change in nature of radial stress near JP was probably due to the local bending of aluminium near JP.

The radial stress at the interface of  $\pm 70^\circ$  and  $\pm 45^\circ$  FRP layer is shown in Figure 7.20. Near JP  $\sigma_{rr}$  was -48 MPa and changes to tensile of 1.8 MPa at the distance of 13 mm from JP.



**Figure 7.19** Radial stress  $\sigma_{rr}$  at the interface of aluminium and epoxy surface



**Figure 7.20** Radial stress  $\sigma_{rr}$  at the interface of  $\pm 70^\circ$  and  $\pm 45^\circ$  FRP layer

## Conclusion

The numerical analysis for Flexural was done for two kinds of specimen under flexural loading conditions, (i) thin sleeve with 80 passes, and (ii) thick sleeve with 150 passes. The first kind of specimen with 80 numbers of passes failed due to breakage of FRP at the joint plane with maximum load of about 370 N. The second kind of specimen made with 150 numbers of passes, was too strong to fail at the joint plane. The specimen failed due to failure of aluminium adherend with the formation of plastic hinge at outside the FRP sleeve. The maximum load taken by the specimen was about 5200 N. Thus, the CFRP sleeve should be strong enough to withstand the load on the specimen that causes the formation of plastic hinge just outside the FRP sleeve. In fact, the FRP joint works well as long as the formation of plastic hinge in the aluminium adherend at the end of FRP sleeve does not take place.

## Scope for future work

The numerical analysis can also be done for torsional loading conditions to check its strength under the same. Numerical analysis of the specimen of CFRP butt-joint can be done by using two different types of materials like steel pipe and aluminium pipe separately to check the compatibility of wetted roving of carbon fiber.

Also, the optimization of the quantity of the wetted roving of carbon or glass fiber used to form a butt-joint may be done and hence the size of the butt joint so formed can be minimized without affecting bending and tensile strength of the FRP butt joint.

## Acknowledgement

I feel happiness in forwarding this paper as an image of sincere efforts. I am very much thankful to my respected guide Prof. Dr. Prashant Kumar who has been a constant source of inspiration. I am also thankful to College of Engineering Pune and MIT College of Engineering for supporting me and guiding me continuously.

## References

- P. Kumar, R. K. Singh, R. Kumar, Joining of Similar and Dissimilar Materials with GFRP, International Journal of Adhesion & Adhesives, Vol. 27, 2007, pp. 68-76.
- R. Kumar, P. Kumar, Joining of Pipes using FRP – an Experimental Study, IE(I) journal – MC, Vol.89,2008
- R. Singh, Characterization of FRP Joints, M.Tech Thesis, IIT Kanpur, Kanpur, 2007.
- R. Verma, Experimental Determination of Flexural and Tensile Strength of the FRP joint, M.Tech Thesis, Govt. College of Engg, Pune, 2008.
- T. EL-Amoury, A. Ghobarah, Seismic Rehabilitation of Beam-Column Joint Using GFRP Sheets, Engineering Structures, Vol. 24, 2002, pp. 1397-1407
- J. M. Lees, Behavior of GFRP Adhesive Pipe Joints subjected to Pressure and Axial Loading, Composite Part A: App. Sc. & Manuf., 2006, in press
- F. L. M. Da Silva, R. D. Adams, The Strength of Adhesively Bonded T-joints, International Journal of Adhesion & Adhesives, Vol. 22, 2002, pp. 311-315.
- M. Kamble, Numerical Analysis to simulate a four-point bend test of FRP-butt joint, College of Engineering Pune 2009.
- T. Jadhav, Numerical Analysis of FRP Butt-joint to determine stress concentration developed in bending and tensile loading, College Of Engineering, Pune 2010
- S. S. Kore, Development and characterization of FRP butt joint, College Of Engineering, Pune 2011.
- R. S. Sabne Experimental study on development and characterization of CFRP butt joint, College Of Engineering, Pune 2012
- B.D. Agarwal and L.J. Broutman, Analysis and Performance of Fiber Composites, Wiley-Inter science Publication, NY, 1980.
- Nye, Physical properties of crystal, oxford university press, London, 1969.
- I. M. Daniel Engineering Mechanics of Composite Materials Oxford University Press Publication, New York, 1994.
- Nikhil Pawar Repairing of cracked thin sheet of aluminium alloy, using CFRP patches through experimental cum numerical techniques College of Engineering, Pune 2013.